

Photocatalysis



An Unexpected Fluctuating Reactivity for Odd and Even Carbon Numbers in the TiO₂-Based Photocatalytic Decarboxylation of C2-C6 Dicarboxylic Acids

Yiran Sun, Wei Chang, Hongwei Ji, Chuncheng Chen, Wanhong Ma,* and Jincui Zhao*^[a]

Abstract: The degradation behaviours of five straight-chain dicarboxylic acids (from ethanedioic acid to hexanedioic acid) were compared in aqueous TiO₂-based photocatalysis. When all other conditions were identical, the degradation rates were found to fluctuate regularly with the parity of the number of carbon atoms. Dicarboxylic acids with an even number of carbon atoms (e-DAs) always degraded more slowly than those acids with an odd number of carbon atoms (o-DAs). This unusual fluctuation in the reactivity for the degradation of dicarboxylic acids by TiO₂-based photocatalysis is very closely related to the different pre-coordination modes of the acids with the photocatalyst. Attenuated total reflection FTIR (ATR-FTIR) of e-DAs labelled with ¹³C showed that both carboxyl groups of the acid coordinate to TiO₂ through bidentate chelating forms. In contrast, only one carboxyl group of the o-DAs coordinated to TiO₂ in a bi-

dentate chelating manner, whereas the other formed a monodentate binding linkage. The bidentate chelating form with bilateral symmetric coordination did not favour degradation. Isotope-labelling experiments were performed with ¹⁸O₂ to observe the different ways in which incorporated oxygen entered the initial decarboxylated products of e- and o-DAs. For the degradation of butanedioic acid, (45.9 ± 0.5)% of the oxygen in the formed propanedioic acid came from H₂O, whereas for pentanedioic acid, (97.4 ± 0.2)% of the oxygen in the formed butanedioic acid came from H₂O. Our results demonstrate that in TiO₂-based photocatalysis, the reactivity of active species, such as [•]OH/h_{vb}⁺, is far from non-selective and that the attacks of these active species on organic substrates are significantly affected by the coordination patterns of the substrates on the TiO₂ surface.

Introduction

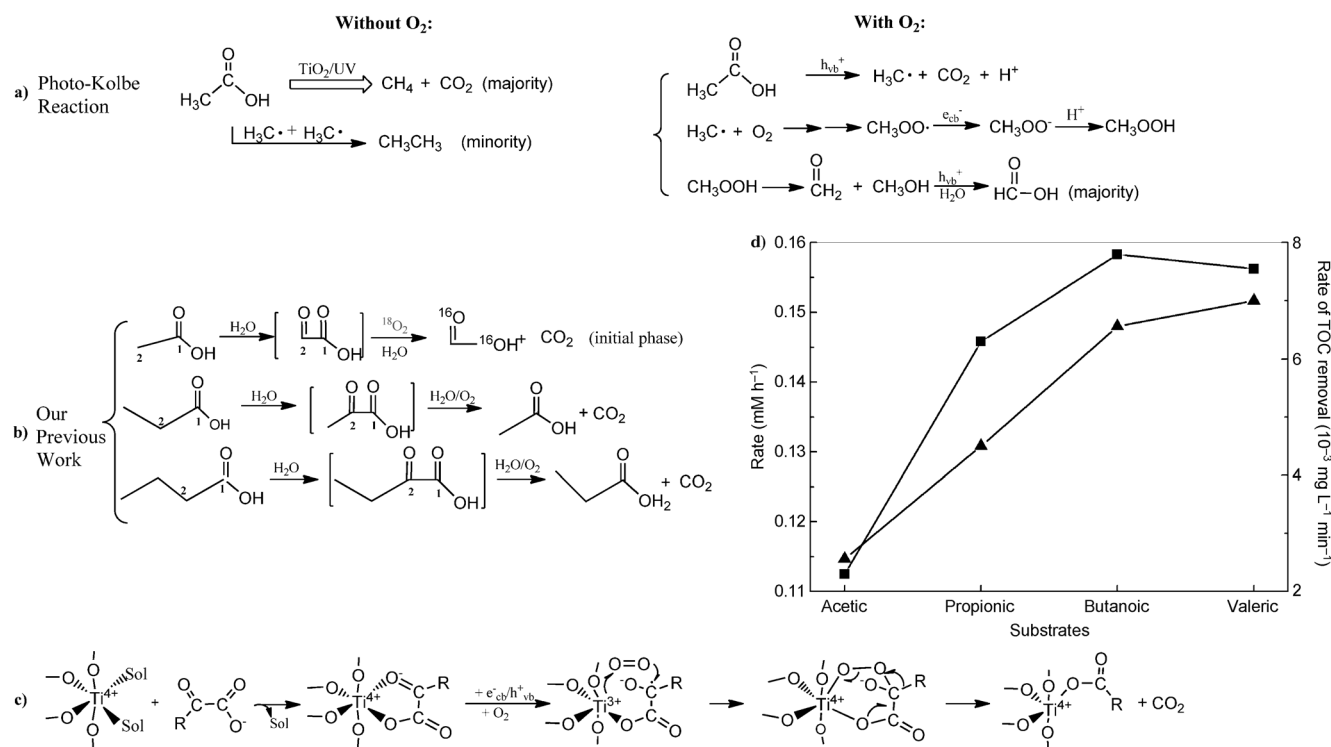
Photo-assisted heterogeneous reactions on TiO₂ particles have attracted much attention because of their promising applications in solar energy conversion, water splitting and treatment of environmental contamination.^[1–3] Under UV irradiation, most surface redox processes are performed by photo-induced electron–hole pairs (e_{cb}⁻/h_{vb}⁺) on the surfaces of the semiconductors.^[4–6] There is a consensus about the initial occurrence of charge separation and recombination of e_{cb}⁻/h_{vb}⁺ on the surface of the semiconductor, but to date insight into, and deep comprehension of, the subsequent induced chemical reactions, especially those involving the cleavage and formation of various chemical bonds, is lacking.^[7,8] For example, in the degradation decarboxylation of organic carboxylic acids in water, the final step by which the organic compounds release CO₂ still remains unclear. Generally, the photo-Kolbe reaction mediated

by e_{cb}⁻/h_{vb}⁺ of a TiO₂ photocatalyst is completely changed by the introduction of dioxygen to the process (Scheme 1a); h_{vb}⁺ begins oxidative decarboxylation to form CO₂ and e_{cb}⁻ participates in *n*–1 RH alkylation in accordance with the cooperative formation mechanism. In the presence of dioxygen, the major decarboxylated product is the *n*–1 acid rather than the *n*–1 hydrocarbon. Acid formation is commonly attributed to the capture of the active alkyl radical by dissolved dioxygen and the subsequent reaction between these species.^[15] From this traditional perspective, the oxygen of the carboxylic group within any formed acid intermediates should have two sources: dioxygen in air and water in the solvent (Scheme 1a, with O₂).

The participation of the latter source of oxygen is possible but is variable because the oxidative hydrolysis of the substrate or the [•]OH radical reaction are involved to different extents, whereas the former source ought to be present in the formed acid product; otherwise, the alkane with the *n*–1 RH product should also be formed in the Kolbe reaction without dioxygen participation. However, our recent work using oxygen-18 labelling^[9] strangely showed that in the formed carboxyl group of the acid there was no oxygen from dioxygen during the initial period. All of the oxygen in the formed acid intermediate came from water in the solvent. The proportion coming from dioxygen gradually increased, however, from 0 to finally ~40% until the reaction had undergone approximately

[a] Y. Sun, Dr. W. Chang, Dr. H. Ji, Dr. C. Chen, Prof. W. Ma, Prof. J. Zhao
Beijing National Laboratory for Molecular Sciences
Key Laboratory of Photochemistry
Institute of Chemistry, Chinese Academy of Sciences
Beijing 100190 (China)
E-mail: whma@iccas.ac.cn
jczhao@iccas.ac.cn

Supporting information for this article is available on the WWW under <http://dx.doi.org/10.1002/chem.201303236>.



Scheme 1. a) Traditional photo-Kolbe reaction with and without dioxygen. b) Our previous observation of the step-by-step cleavage of the C₁–C₂ bonds of monocarboxylic acids. c) A possible pre-coordination process allowing the incorporation of dioxygen into the product during the decarboxylation of α -keto acids. Right inset: average rates of degradation as a function of number of carbon atoms for both full conversion (■) and total organic carbon (TOC) removal (▲) of the four monocarboxylic acids by TiO₂-based photocatalysis. The initial concentrations of the four acids were 2 mM in a volume of 30 mL, and the surface area of the P25 film was 6 cm² in all experiments.^[3,9,10–16]

50% conversion (Scheme 1 b, acetic acid case). Coincidentally, the hydroxylation of benzene and benzoic acids by photocatalysis with TiO₂ also revealed that the oxygen composition in the formed phenol from H₂¹⁸O decreased as the conversion increased.^[9,17] For a single product, this variation of the oxygen source with reaction progress strongly indicated that the reaction of the substrate with the active species, such as $\cdot\text{OH}$ radicals and O₂⁻/ $\cdot\text{OOH}$ radicals, was not unalterable as presumed by the traditional view of diffusive control. A reasonable explanation for such an alternation could be competitive reactions controlled by changes in the interactions between the TiO₂ surface sites and the substrates (including solvents such as H₂O), intermediates and products. Different coordination potentials for the substrates with the TiO₂ surface sites might play a key role in revealing the initial reactions with e_{cb}⁻/h_{vb}⁺. Indeed, our IR experiment with H₂O and O₂ labelled with the oxygen-18 isotope identified an α -keto acid intermediate, a common precursor shared by subacids, an intermediate that emerged during the degradation of aliphatic straight-chain monocarboxylic acids.^[9] Tentatively, an underlying bidentate coordination^[9] of the nascent α -keto acid intermediate with Ti sites was proposed to be the most convenient precursor to aid in the incorporation of dioxygen into the split of C₁–C₂ bond, likely through a Crigee rearrangement^[18] (Scheme 1 c). The carboxylic acids with shorter carbon chain lengths, such as acetic acid, should show slower degradation than those with longer chains, such as propanoic acid. This effect was attributed to

greater difficulty of converting the methyl group of acetic acid into the required α -keto acid intermediate than the methylene group of propanoic acid. However, for aliphatic straight-chain monocarboxylic acids with four or more carbon atoms, there were no significant differences in their decarboxylation rates because of the similarities in both the reactivity of the methylene group and the coordination of the α -keto acid to TiO₂ (right inset of Scheme 1).

In previous work, there are almost no exceptions to the dependence of the decarboxylation process on the carbon chain length for the degradation of straight-chain monocarboxylic acids (as described by the inset in Scheme 1).^[9] Such a unidirectional dependence of the transformation on the number of carbon atoms suggests that the formation of the α -keto acids or the coordination of these acids with the TiO₂ surface plays a key role to dictate the $\cdot\text{OH}$ radical/h_{vb}⁺ breaking of the C₁–C₂ bond of the initial acids. Additionally, one end of the carboxylic group exclusively chelates with TiO₂ and prevents the remote C–C or C–H bonds at the other end of the acid from accessing the active species of TiO₂. In particular, such coordination by a monocarboxylic donor allows only the α -C–H bond of the acid to be preferentially oxidised; therefore, the cleavage of every C₁–C₂ bond of the acid takes place step-by-step (see Scheme 1 b). Consequently, every inferior acid is always a monocarboxylic acid rather than a dicarboxylic acid, aldehyde acid or hydroxyl acid. In this way, is the degradation always linearly dependent on the number of carbon atoms if the substrates

have multiple coordinative groups within a straight chain? Is the reactivity of TiO_2 -based photocatalysis of a straight-chain dicarboxylic acid, for example, the simplest case of multiple coordination sites, similar to that of straight-chain monocarboxylic acids? Few theoretical predictions and little experimental evidence have been reported on this issue.

Analogous to the studies of the degradation of monocarboxylic acids by TiO_2 -based photocatalysis,^[9] in this work, a range of dicarboxylic acids will be employed (from ethanedioic to hexanedioic acid) to investigate their degradation behaviours. Some excellent studies have been performed to compare the adsorption of dicarboxylic acids, including ethanedioic (oxalic), propanedioic and butanedioic acid, on the surface of TiO_2 under dark conditions.^[19,20] The role of adsorption modes in photocatalytic events was also reported in relation to butanedioic acid and its mono- and di-hydroxyl derivatives.^[20b] In essence, decarboxylation required direct carboxylic group– TiO_2 contact.^[19b] Most characterisation results from attenuated total reflection (ATR-FTIR) spectra indicated that oxalic acid typically exhibited bidentate coordination by both of the carboxyl groups on the TiO_2 surface, whereas propanedioic acid was significantly different from oxalic acid, in that one carboxyl had bidentate coordination and the other had monodentate coordination with the TiO_2 .^[20] Inspired by these fine characterisation studies, in this work we systematically correlate the photocatalytic transformation and mineralization of dicarboxylic acids with the different pre-coordination patterns on the TiO_2 surface. An unusual oscillating reactivity is revealed for dicarboxylic acids as a function of the number of carbon atoms. Through ATR-FTIR spectra of dicarboxylic acids with the ^{13}C isotope as well as the performance of degradation experiments with isotopically labelled $^{18}\text{O}_2$, we examine whether the same bidentate binding with the TiO_2 surface by two carboxyl groups determines whether dioxygen or H_2O participates in the splitting, induced by $e_{\text{cb}}^-/h_{\text{vb}}^+$, of $\text{C}_1\text{--}\text{C}_2$ bond(s). Our results demonstrate the importance of understanding the pre-coordination of substrates with TiO_2 and the effect of this pre-coordination on the roles of dioxygen and $\cdot\text{OH}/h_{\text{vb}}^+$ in photocatalytic reactions.

Results and Discussion

Typical fluctuating reactivity as a function of number of carbon atoms for straight-chain dicarboxylic acids

To determine the nature of the decarboxylation process by TiO_2 -based photocatalysis as generally as possible, we selected five straight-chain dicarboxylic acids (from oxalic acid to hexanedioic acid) to systematically compare their reactivities in identical aqueous solutions. The changes in the concentration of every substrate and generated intermediate during the course of the reaction were measured by ion chromatography (IC) at optimum conditions (see the Experimental Section and Figure 4 for details). Figure 1 gives the average rate for full conversion of every dicarboxylic acid as a function of the number of carbon atoms under identical reaction conditions.

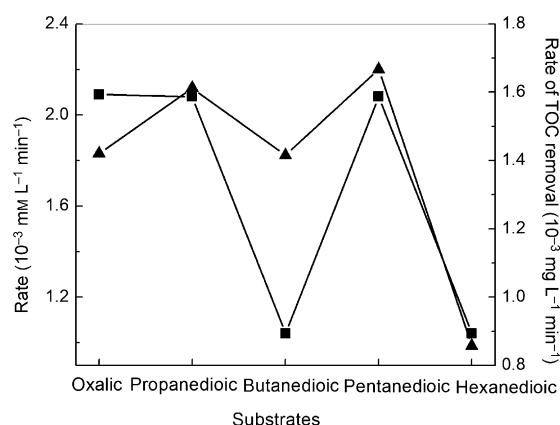


Figure 1. Average rates for both full conversion (■) and TOC removal (▲) by TiO_2 -based photocatalysis for the five dicarboxylic acids as a function of their carbon number. The initial concentration of every acid was 0.5 mM in a volume of 50 mL, and 25 mg of P25 TiO_2 was added. P25 TiO_2 was pre-treated according to the method described in ref. [23]. Similar to our prior work on carboxylic acids,^[9] the pH value of each acid solution was not adjusted during the reaction period.

In sharp contrast to the linear carbon-number-dependent reactivity of monocarboxylic acids (inset of Scheme 1), the degradation rates of dicarboxylic acids showed an abnormal fluctuation as the carbon number increased. Those species with an odd number of carbon atoms (o-DAs) degraded faster than those with an even number of carbon atoms (e-DAs). The degradation of oxalic acid was somewhat faster than expected because of the auto-decomposition of oxalic acid under UV irradiation.^[21] Although every dicarboxylic acid had different intermediates (Table 2) and these intermediates probably affected the transformation rates of the initial substrates, every single dicarboxylic acid maintained this fluctuated reactivity until total transformation. This peculiar aspect of the degradation reminded us to simultaneously observe the CO_2 formation rate as a function of the carbon number of the substrates (Figure 1). Surprisingly, the fluctuation pattern described by CO_2 formation was perfect even for oxalic acid.^[21] The order of mineralization for dicarboxylic acids is clearly completely different from that of monocarboxylic acids in TiO_2 -based photocatalysis. In principle, the decarboxylation of organic acids followed the direct single-step reaction of h_{vb}^+ oxidation described by the photo-Kolbe reaction mechanism.^[9,12–16] If the other conditions were the same, consequently, the h_{vb}^+ yield was constant; thus, the time required for full decarboxylation per carboxylic group should be the same. The longer the carbon chain of the acid was, the longer the time required was for full mineralization. This case was similar to most homogeneous oxidations that have been examined (see the next section on $\text{S}_2\text{O}_8^{2-}$ photooxidation). However, this fundamental inference had never been clearly displayed by the degradation of straight-chain monocarboxylic acids in TiO_2 -based photocatalysis. Quite the opposite was true; the sequence of reactivity was acetic acid < propionic acid < butanoic acid < pentanoic acid (inset of Scheme 1). This result at least illustrated that radical oxidation by $\cdot\text{OH}/h_{\text{vb}}^+$ was neither the control step of decarboxylation nor the chief contributor to the decarboxylation

of monocarboxylic acids in the heterogeneous system. This opposite trend in reactivity relative to homogenous oxidation indicated that the surface sites of the catalyst play a crucial role. The formation of the α -keto acid followed by bidentate chelating coordination on the TiO_2 surface was thought most likely to determine the rate of the degradation of monocarboxylic acids.^[9] However, the degradation of dicarboxylic acids seemingly did not follow the mechanism of either homogenous or heterogeneous TiO_2 -based photocatalytic oxidation of monocarboxylic acids. To our knowledge, the consistent fluctuation patterns for the rates of substrate transformation and CO_2 formation as a function of the alternation between odd and even carbon numbers has never been reported or attracted attention. Apparently, this unique reactivity, compared with the degradation of monocarboxylic acids, arose exclusively from the addition of another carboxylic group.^[20b,c] There are two possible ways that a dicarboxylic acid can cause such an oscillation in reactivity as a function of the carbon number: i) through the variety of inherent redox nature of dicarboxylic acids with the carbon chain fluctuations; ii) through significantly different coordination modes of substrates with odd and even carbon numbers with the TiO_2 surface. The former was easily excluded by the following control experiments. Thus, it is likely that the two carboxylic units in dicarboxylic acids bind to the TiO_2 surface and dramatically alter the conventional route, namely that active species, such as $\cdot\text{OH}$ radical/ h_{vb}^+ , dominate TiO_2 -based photocatalysis.

$\text{S}_2\text{O}_8^{2-}$ photooxidation

$\text{S}_2\text{O}_8^{2-}$ photooxidation is a classic one-electron-oxidation process that takes place through homogenous cleavage of $\text{S}_2\text{O}_8^{2-}$ into the highly active $\text{SO}_4^{\cdot-}$ radical under UV light and is usually used to degrade organic pollutants in water.^[22] The oxidative activity of the $\text{SO}_4^{\cdot-}$ radical is so high that once formed, the $\text{SO}_4^{\cdot-}$ radical reacts quickly with the substrate regardless of the redox potential of the substrate. Therefore, for this homologous oxidation, the time for the entire transformation process for an equivalent of any substrate, that is, the average conversion rate, definitely depended on the length of the carbon chain of the substrates. The concentration changes during the course of the reactions of five dicarboxylic acids were measured by IC. Figure 2 illustrates the average rates for both the complete conversion and the mineralization of the five dicarboxylic acids as a function of carbon number during $\text{S}_2\text{O}_8^{2-}$ photooxidation. The average degradation rates of the five dicarboxylic acids decreased almost linearly as the carbon number increased (except for oxalic acid), whereas the average mineralization rates slowed significantly as the carbon number increased. The correlation of both the degradation and the mineralization with the carbon number of the substrates was different from that seen in the TiO_2 -based photocatalysis. Additionally, the features did not agree with the degradation of monocarboxylic acids by TiO_2 -based photocatalysis either. This dependence between the reactivity and the carbon chain length of the substrate demonstrated that the formation of $\text{SO}_4^{\cdot-}$ and the subsequent reactions in homogenous solutions

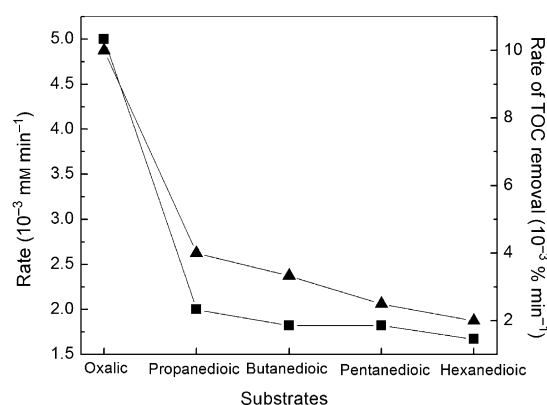
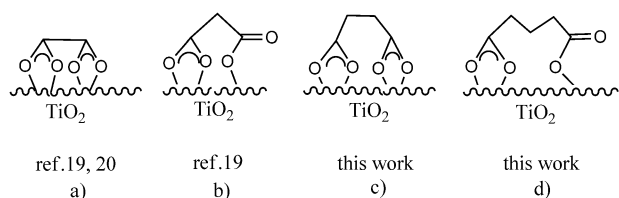


Figure 2. Average rates for both full conversion (■) and TOC removal (▲) of five dicarboxylic acids by $\text{S}_2\text{O}_8^{2-}$ photooxidation as a function of carbon number. The initial reactive solution (50 mL) for the degradation of each dicarboxylic acid sample contained 0.5 mM dicarboxylic acid and 15 mM $\text{K}_2\text{S}_2\text{O}_8$.

were not influenced by any properties of the substrate except for the carbon number. Furthermore, this suggested that the coordination of the substrates to the TiO_2 surface altered the oxidation sequence despite the fact that the oxidising species such as the $\cdot\text{OH}$ radical/ h_{vb}^+ were more powerful than the $\text{SO}_4^{\cdot-}$ radical and could react with the substrate very fast. Thus, we tentatively attributed this fluctuating reactivity to the differences in the pre-coordination states of the two carboxylic groups on the TiO_2 surface between e-DAs and o-DAs.

Nature of pre-coordination of dicarboxylic acids on the TiO_2 surface

Intrinsically, the coordination model was correlated with the distribution of the electronic charge density of the whole molecule and this distribution had great impact on the oxidative degradation of the molecule. The carboxylic groups at both ends of dicarboxylic acid molecules made the location of the framework of the molecule on the surface of the TiO_2 conspicuously different from that of the monocarboxylic acids.^[19,20] However, this difference could not account for the regular fluctuations in reactivity with the odd and even carbon number of the homologues. It has been reported that the coordination models for the two terminal carboxylic groups with TiO_2 could be identical or different, based on the carbon number of the dicarboxylic acid.^[19] For example, ATR-FTIR results indicated that both of the carboxylic groups of oxalic acid formed a bidentate chelating mode with TiO_2 , whereas only one carboxylic group of propanedioic acid formed a bidentate chelating mode and the other carboxylic group formed a monodentate bridge to a TiO_2 site (Scheme 2a and b). To obtain more detailed results for the adsorption states on the TiO_2 surface for all five dicarboxylic acids, we carefully studied the pre-coordination states of butanedioic and pentanedioic acid on the TiO_2 surface by using ATR-FTIR.^[19,20] Figure 3a shows the ATR-FTIR spectrum of pentanedioic acid and the IR spectrum of pentanedioic acid in solution, and Figure 3b shows the ATR-FTIR spectrum of butanedioic acid and butanedioic acid with ^{13}C la-



Scheme 2. Two modes of adsorption characterized by bidentate chelation and mono-/bidentate chelation with the TiO_2 surface for e-DAs and o-DAs, respectively.

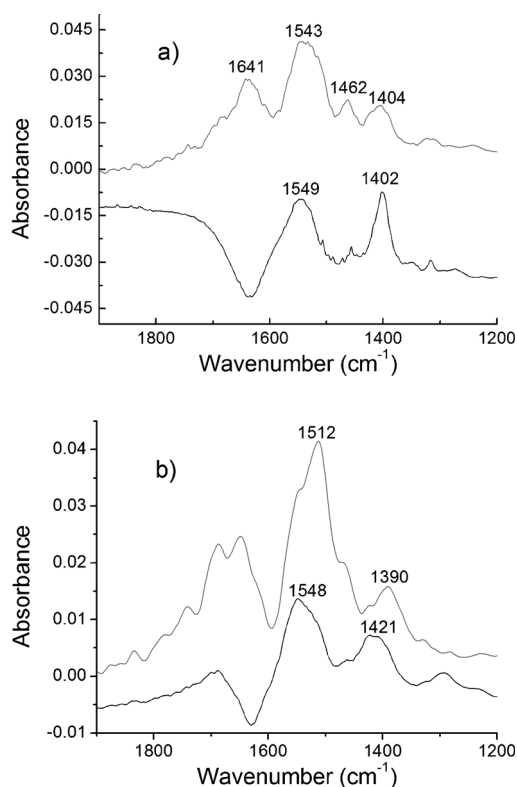


Figure 3. ATR-FTIR spectra of a) pentanedioic acid in solution (bottom) and adsorbed on the surface of TiO_2 film (top) and b) normal butanedioic acid (bottom) and butanedioic acid labelled with ^{13}C on both carboxyl groups (top). The concentration of the substrates was 5 mm, except for the pentanedioic acid in solution (a, bottom) the concentration of which was 0.02 mm.

belling. In Figure 3a (bottom), the $\nu_{\text{as}(\text{COO}^-)}$ and $\nu_{\text{s}(\text{COO}^-)}$ for a sample of dissolved pentanedioic acid (on the ZnSe substrate) are 1549 and 1402 cm^{-1} , respectively, in the normal IR spectra; thus, $\Delta_{\text{as}} = 147 \text{ cm}^{-1}$, where ν_{as} and ν_{s} stand for the wavenumbers of the asymmetric and symmetric vibration of dicarboxylic acid, respectively. However, in the ATR-FTIR spectrum of pentanedioic acid (adsorbed on the coated TiO_2 film), four peaks appeared, at 1641, 1543, 1462 and 1404 cm^{-1} , indicating different chemical adsorption of two carboxylic groups and TiO_2 surface. In these peaks, two pairs of carboxylate vibrations undoubtedly belonged to different binding patterns. Therefore, two different combinations were possible for the Δ_{sy} values: either 237 and 81 cm^{-1} or 179 and 139 cm^{-1} .

Regardless of which pair was true, the values indicated that $\Delta_{\text{as}} > \Delta_{\text{sy}}$ and $\Delta_{\text{as}} < \Delta_{\text{sy}}$; Δ_{sy} where stands for the difference of ν_{as} and ν_{s} in dissolved solution on the TiO_2 film, while Δ_{as} stands for the difference of ν_{as} and ν_{s} in dilute solution on the ZnSe substrate. Thus, the two carboxylic groups in pentanedioic acid were adsorbed on the TiO_2 surface with one group bidentate ($\Delta_{\text{as}} > \Delta_{\text{sy}}$) and one group monodentate ($\Delta_{\text{as}} < \Delta_{\text{sy}}$; Scheme 2d). Similarly, Dolamic et al. reported that the adsorption mode for the two carboxylate groups in propanedioic acid on the TiO_2 surface is with one group bidentate and the other group monodentate (Scheme 2b).^[19,20,24] As shown in Figure 3b, butanedioic acid with a different initial concentration to that previously applied by others was first used to carry out ATR-FTIR experiments. Distinctly opposite to the case of pentanedioic acid, there were only two peaks, 1548 and 1421 cm^{-1} , that appeared as chemical adsorption of the carboxylic groups. This indicated that the two carboxylic units of butanedioic acid adopted a single chelating mode when bound to TiO_2 . To confirm that the two peaks belong to the carboxylic group adsorption, ^{13}C isotopically labelled butanedioic acid (in which the two carbon atoms of the carboxyl groups were labelled) was employed in ATR-FTIR experiments. On the substitution of the ^{13}C atoms, ν_{COO} changed in accordance with Hooke's law. Accordingly, we identified that the peaks at 1548 and 1421 cm^{-1} of the normal butanedioic acid and the peaks at 1512 and 1390 cm^{-1} of the ^{13}C -labelled butanedioic acid belonged to the asymmetric and symmetric stretching vibrations of COO^- , respectively. The difference between the two carboxylate stretching modes, that is, $\nu_{\text{as}(\text{COO}^-)}$ and $\nu_{\text{s}(\text{COO}^-)}$, was 127 cm^{-1} represented by Δ_{sy} . According to well-established experimental and theoretical calculations,^[20,24] the difference for butanedioic acid free in solution is 157 cm^{-1} , represented by Δ_{as} , and it was smaller than the former difference (127 cm^{-1}). This difference signified that both of the carboxylate groups coordinated to TiO_2 through the same bidentate chelating mode (Scheme 2c).^[20,24] Similar to the pentanedioic acid case, the peak at 1716 cm^{-1} was assigned to the physical adsorption of the carboxylic group. To confirm these adsorption characteristics, we carried out ATR-FTIR measurements of pentanedioic acid and butanedioic acid for high initial concentrations (in the range 0.05 mm to 100 mm; Figure S1 in the Supporting Information). All of the features were in agreement with the results in Figure 3, except for the peak at 1712 cm^{-1} for pentanedioic acid (Figure S1b; 1690 cm^{-1} for butanedioic acid, Figure S1c) that appeared as a non-dissociated $-\text{COOH}$ vibration absorbance peak at high concentration. In particular, the ATR-FTIR spectra of ^{13}C -labelled butanedioic acid with a different initial concentration (Figure S1d) showed only two peaks, 1512 and 1390 cm^{-1} , very similar to the low-concentration spectra in Figure 3b, indicating that the symmetrically bidentate chelating mode remained largely unchanged with over-loading of the butanedioic acid on the surface of the TiO_2 film. Thus, all the e-DAs clearly had their two carboxylic groups adopt the same bidentate coordination pattern, whereas those of o-DAs differed, with one group adopting monodentate coordination and the other group adopting bidentate coordination with the TiO_2 surface (Scheme 2). Our investigations into the coordina-

tion of dicarboxylic acids with the TiO₂ surface agreed with previous work concerning the adsorption in the dark of dicarboxylic acids on TiO₂,^[19,20] ZnO,^[25] and other oxides.^[24] For the substrates, this alternating coordination as a function of odd or even carbon number perfectly agreed with the regular fluctuations in the degradation rates. All of the e-DAs degraded more slowly than the o-DAs. That is, both oxidative degradation and mineralization of dicarboxylic acids with symmetric bidentate chelating coordination were more difficult than these processes for acids with asymmetric coordination. Next, we will look further at the details of the differences in the cleavage of the C₁–C₂ bond of the dicarboxylic acids with even and odd carbon numbers through oxygen-18 isotope-labelling experiments (¹⁸O₂/H₂¹⁶O). By identifying differences in the incorporated oxygen-18 in the initial decarboxylation products for dicarboxylic acids with even and odd carbon numbers, we expected to determine which attack, namely H₂O/h_ν⁺ or O₂/e_{cb}⁻, was significantly affected by the two different coordination environments.

Comparison of photocatalytic degradation products between pentanedioic and butanedioic acid by oxygen-18 isotope-labelling experiments

To describe the relationship between the reactivity and coordination environment during the TiO₂-based photocatalytic reaction in detail, butanedioic and pentanedioic acids were chosen for isotope-labelling experiments with ¹⁸O₂ (95%) to observe the ¹⁸O distribution in the product after elimination of one carbon atom (Table 1).

Blank experiments were performed to examine the oxygen exchange between the carboxyl groups of the dicarboxylic acids and ¹⁸O₂ and these showed that such exchange was negligible (see the Supporting Information, Figure S2). In addition, similar to the exchange between monocarboxylic acids and H₂¹⁸O,^[9] the product acids formed with ¹⁸O did not exchange with H₂¹⁶O (see the Supporting Information, Figure S3). This was in very good agreement with earlier studies in both homo- and heterogeneous systems^[9,26] in which little oxygen exchange took place between dioxygen and any carboxyl, aldehyde or alcohol groups. Therefore, we considered the results from ¹⁸O₂/H₂¹⁶O where the *n*–1 degradation products of dicarboxylic acid were analysed by GC-MS (Table 1).

Table 1 shows the respective oxygen isotopic proportion in the produced dicarboxylic acid, which had one carbon atom

less than the parent dicarboxylic acid. In the formed *n*–1 dicarboxylic acid molecule, one carboxylic group was considered to be new, whereas the other group was classed as the original group. The e- and o-DA showed a striking contrast in the way H₂O/dioxygen were combined into their corresponding *n*–1 dicarboxylic acids; nearly all ([97.4 ± 0.2]%) oxygen came from H₂O for the degradation of pentanedioic acid, whereas (45.9 ± 0.5)% came from H₂O in that of butanedioic acid. In spite of some disputes about the way in which dioxygen/H₂O participates in the degradation,^[9,17,23,27–29] the results for different oxygen sources in the formed carboxylic groups unambiguously indicated the competition between activated H₂O/h_ν⁺ and O₂/e_{cb}⁻. The asymmetrically chelating donor of the o-DA favoured activated H₂O/h_ν⁺ attack, whereas the symmetric coordination model of e-DAs, such as butanedioic acid, significantly favoured attack by dioxygen. The asymmetrically chelating o-DA favoured ·OH radical/h_ν⁺ decarboxylation; therefore, the degradation of these e-DAs was faster than that of symmetrically chelating o-DAs. This result entirely agreed with the fluctuating degradation rates for e- and o-DAs.

Identification of a possible degradation process

In our previous work on the degradation of straight-chain aliphatic monocarboxylic acids,^[9a] the step-by-step C₁–C₂ bond cleavage dominated throughout the photocatalytic process. Every secondary monocarboxylic acid (*n*–1, *n*–2 and *n*–3) was formed, and no dicarboxylic acid products were observed. Therefore, the degradation of the monocarboxylic acid began neither from the end of the alkyl group nor with the cleavage of any other C–C bond. This result strongly indicated that the attack of either ·OH radical (activated H₂O by h_ν⁺) or dioxygen (activated by e_{cb}⁻ or organic radical R[·])^[27] exclusively began at the end with the coordinating carboxylic group. In the present work, we also tried to identify the degradation products as much as possible for every dicarboxylic acid by using IC (Figure 4). The detailed results are summarized in Table 2. We expected to find more evidence to support the established relationship between the coordination pattern (especially based on the even or odd carbon number of the dicarboxylic acids) and the breakage of any C₁–C₂ bond in the presence of multiple chelating coordination modes. Firstly, oxalic acid was generated during the degradations of all the other dicarboxylic acid substrates but did not become the major product, partly because it was too unstable to accumulate. Secondly, in the

Table 1. Distribution of ¹⁸O₂ isotope in the products formed from pentanedioic and butanedioic acid degradation by TiO₂ in H₂¹⁶O solution under an ¹⁸O₂ atmosphere.

O isotopomers ^[a] [%]	¹⁶ O 97.4 ± 0.2	¹⁸ O 2.6 ± 0.3	¹⁶ O 45.9 ± 0.5	¹⁸ O 54.1 ± 0.6
[a] The calculation assumed that one of the carboxyl groups of the produced butanedioic acid or propanedioic acid was inherited from the parent pentanedioic acid or butanedioic acid without any change. The difference in the distribution of oxygen isotope appeared only in the other carboxyl group.				

Table 2. Distribution of products and their maximum concentrations during TiO₂-based photocatalytic degradation of five dicarboxylic acids.

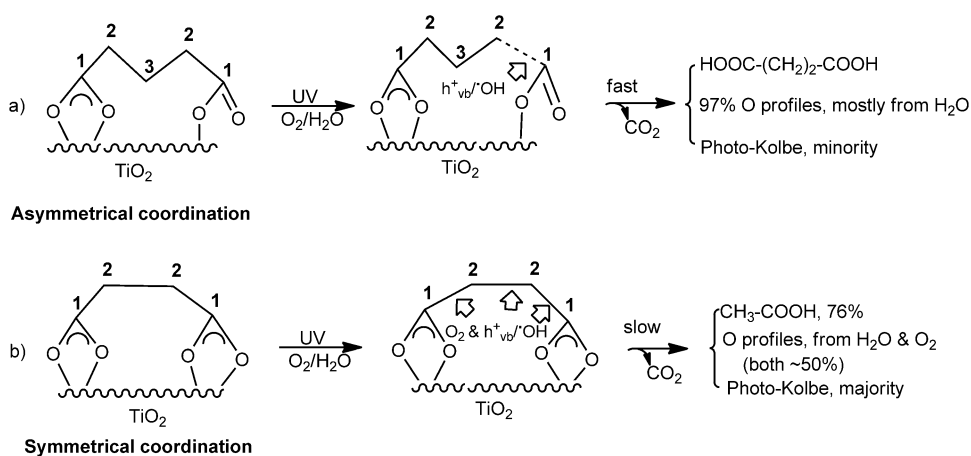
Initial conc. 0.5 mM	e-DAs		Initial conc. 0.5 mM	o-DAs	
	Major products	Max. conc. [mM]		Major products	Max. conc. [mM]
oxalic acid	formic acid	0.060	propanedioic acid	acetic acid	0.241
	acetic acid propanedioic acid	0.065 0.041		propanoic acid	0.077
butanedioic acid	acetic acid	0.380	pentanedioic acid	acetic acid	0.185
	propionic acid oxalic acid	0.132 0.026		propanoic acid propanedioic acid	0.243 0.014
	propanedioic acid	0.090		butanedioic acid	0.077
hexanedioic acid	propanoic acid	0.218			

degradation of elementary dicarboxylic acids, such as oxalic and propanedioic acids, there were small amounts of either dicarboxylic acid products with larger carbon numbers or some monocarboxylic acid products with the same carbon number as the initial substrate. Namely, propanedioic and acetic acid were produced in the oxalic acid degradation, and propanoic acid was produced in the propanedioic acid degradation. This result was in agreement with the extension of the carbon chain through CO₂ radical or other carbon-centred radical addition reactions.^[15] However, generally speaking, these products were in very low yields. During the degradation process of all of the five dicarboxylic acids, none of the mono- or dicarboxylic acid intermediates formed had undergone substitution at any site of the carbon chain. Similar to the serial degradation of monocarboxylic acids,^[9a] dicarboxylic acids were not seen to oxidize any other C–H or C–C bond except for the C₁–C₂ bond. In addition, mono- or dicarboxylic acid products that had lost only one carbon atom were observed in the degradation of all five initial dicarboxylic acids. The generation of the *n*–1 monocarboxylic acid was significant, and it should arise from the reduction of the alkyl radical by proton-coupled e_{cb}[–] transfer or by hydrogen abstraction; this result clearly demonstrates that e_{cb}[–] and h_{vb}⁺ simultaneously induced different chemical reactions. More importantly, there was a notable tendency in e-DAs to form or accumulate monocarboxylic acids from cleavage at the middle position of the

carbon chain. For example, the maximum yield of acetic acid was approximately 76% in the butanedioic acid degradation, and the maximum yield for the sum of propanoic acid and acetic acid was 90% in the transformation of hexanedioic acid (Table 2). Despite this, these degradation products for o-DAs had yields of no more than 50%. Apparently, during the noncarboxylic acid degradation, the latter case was more coincident with that from the step-by-step cleavage of the C₁–C₂ bond to form acids without the selectivity. Given that the formation of monocarboxylic acids exclusively originated from the photo-Kolbe reaction, it could be speculated that when one component became a major product, the cleavage of another C–C bond, for example, C₂–C₃ for butanedioic acid or C₃–C₄ for hexanedioic acid, was likely to become the predominant process. In addition, the C₁–C₂ bonds of the symmetrically chelating e-DAs broke with more difficulty than those of the asymmetrically chelating o-DAs (Scheme 3). We believe that the weaker monodentate coordination of the carboxyl group favoured approach and attack by the

underlying oxidant. Even dioxygen, as a weakly coordinating and attacking ligand on the TiO₂ surface, had a fairly high efficiency, a fact that was shown by the oxygen isotope labelling in the products.

Such a carbon-number-dependent reactivity is fundamental to understanding the most basic oxidative reactions of substrates by [•]OH radical/h_{vb}⁺ and by dioxygen (Scheme 3). Traditionally, for homologues, the rates of degradation were thought to correlate with the redox potential in the homogeneous solution based on the Marcus equation.^[30] Otherwise, if substrates had similar redox potentials or if the oxidant species were active enough, such as the SO₄^{•–} radical, the rates depended on the carbon number. Almost no reports concerned with coordination on the TiO₂ surface noted the significant induced regular fluctuations in reactivity related to the odd and even carbon numbers. Of course, there are still many uncertain



Scheme 3. Schematic diagrams of photocatalytic degradation. a) Pentanedioic acid represents the dicarboxylic acids with an odd number of carbon atoms and b) butanedioic acid represents the dicarboxylic acids with an even number of carbon atoms.

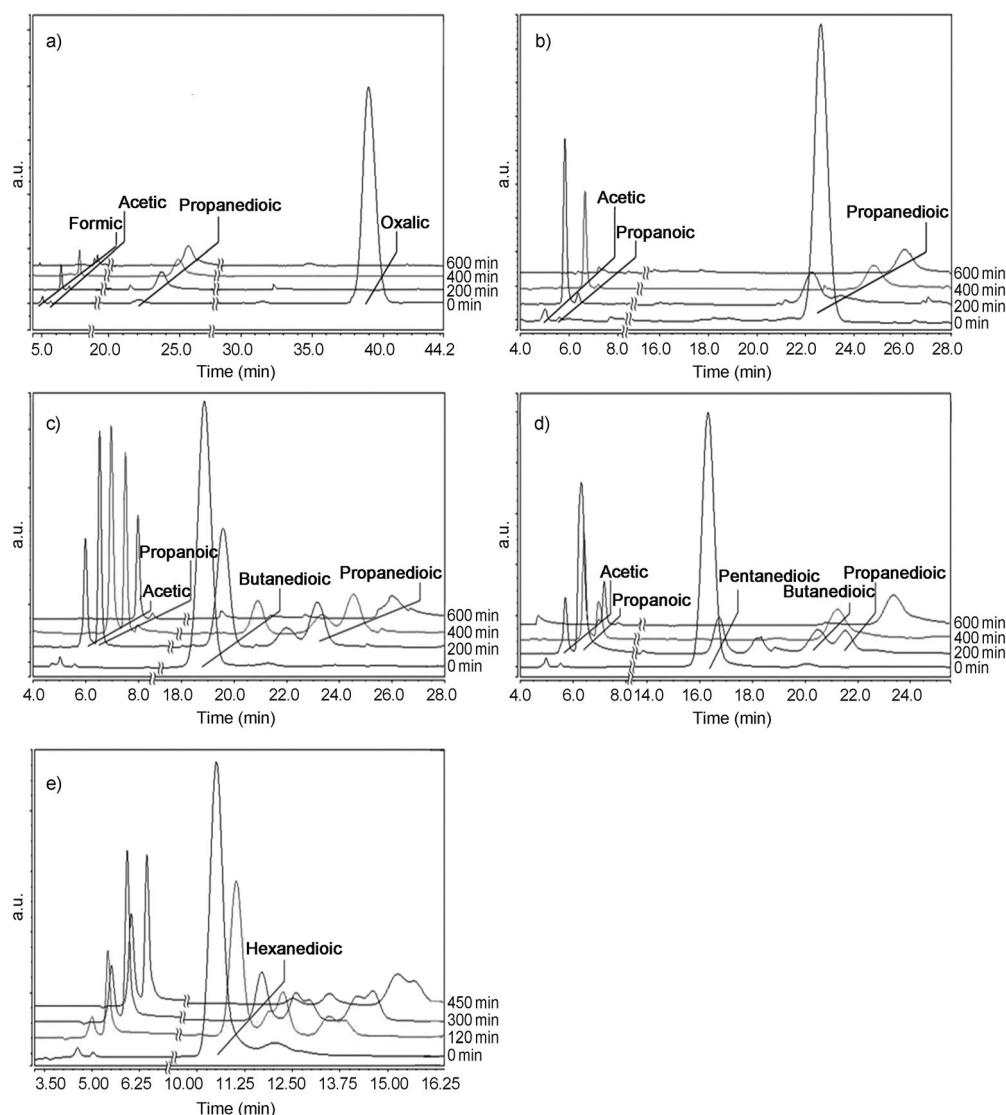


Figure 4. IC spectra of a) oxalic acid, b) propanedioic acid, c) butanedioic acid, d) pentanedioic acid and e) hexanedioic acid during photocatalytic degradation. Degradation times are marked on the right-hand side of each graph and the retention time of every sample are marked on the bottom of the graph.

interactions among the chelating groups of the substrates or the intermediates, moieties remote from the anchored active sites, and subsequent active species, and these interactions require investigation with more direct methods to observe single-molecular behaviour in situ on the TiO_2 crystal facet.^[31]

Conclusion

We revealed a peculiarly fluctuating reactivity for straight-chain dicarboxylic acids with even and odd carbon numbers (e-DAs and o-DAs) in aqueous solution under TiO_2 -based photocatalysis. Among the five dicarboxylic acids investigated (from oxalic acid to hexanedioic acid), all of the o-DAs degraded faster than the e-DAs when the photocatalytic conditions were controlled to be identical. This odd/even dependence strongly differed from the characteristics for $\text{S}_2\text{O}_8^{2-}$ homogenous oxidation and for TiO_2 -based photocatalytic degradation of a series of

straight-chain monocarboxylic acids. Our results demonstrate that the traditional insight that $\cdot\text{OH}$ radicals/ $h_{\nu\text{b}}^+$ oxidise substrates fast is only associated with redox property or total carbon number and cannot be compared with TiO_2 -based photocatalysis at all. Through ATR-FTIR experiments and isotope-labelling methods, we showed that the differences in coordination patterns determined whether selective cleavage of the C_1 – C_2 bond of the dicarboxylic acids was predominant. The two carboxyl groups for e-DAs adopted symmetrical bidentate chelation to the TiO_2 surface. This strong coordination meaningfully restrained any approach or attack by an active species, partly because this coordination model led to C_1 – C_2 bond electron deficiency, which inhibited oxidative cleavage. On the other hand, o-DAs exhibited asymmetrical chelation, which permitted all oxidant species, even dioxygen, to approach and attack the weakened C_1 – C_2 bond associated with the monodentate chelation and thereby greatly enhanced degradation and mineralisation. All of our results clearly illustrate that the coordination characteristics of the substrates' functional groups with the TiO_2 surface are very important and are sometimes the main factor that

determines the active species, such as $h_{\nu\text{b}}^+/\cdot\text{OH}$ radical and O_2 , targeted attack on the C–C or C–H bond of the substrates.

Experimental Section

Catalyst and chemicals

Both C1-C6 monocarboxylic acids and C2-C6 dicarboxylic acids were obtained from Alfa Aesar. A silylating reagent consisting of bistrimethylsilurea (BSU) and hexamethyldisilazane (HMN) was bought from Acros. All the chemicals were of analytical-grade purity and were used as received. $^{18}\text{O}_2$ was purchased from Cambridge Isotope Laboratories, Inc. The isotopic enrichment was 95%. H_2^{18}O was purchased from Jiangsu Changshu Chemical Limited. The isotopic enrichment was 96%, as determined by mass spectrometry.

Degussa P25 TiO_2 , containing 80% anatase and 20% rutile phases with a surface area of $50\text{ m}^2\text{ g}^{-1}$ and an average primary particle

size of 25 nm, was used in the photo-assisted reactions. Before every experiment, P25 was pre-treated according to the method described in ref. [23].

Instrumentation

The photocatalytic process was analysed by ion chromatography (IC) and total organic carbon analysis (TOC). Samples of 2.5 mL were removed and filtered at regular time intervals during the irradiation, and 0.3 mL of the samples were analysed by IC. The concentrations of carboxylic acids and dicarboxylic acids were measured by a DX-900 Ion Chromatograph with an IonPac AS23 column (Dionex). The eluent for IC used 13 mM KOH solution. The flow rate was 0.7 mL min⁻¹. The identification of the intermediates by IC was performed by comparing the retention times with those of standards. The remaining 2.2 mL solution was used for TOC. TOC was measured by using a Tekmar Dohrmann Apollo 9000 TOC Analyser.

GC-MS analyses were performed with a Finnigan Trace GC ultra gas chromatograph with a 25 m DB-5 column, coupled with a Finnigan Trace DSQ mass spectrometer. The injector port was set for split operation at 250 °C. The temperature program of the column was as follows: hold at 50 °C for 4 min, then the temperature was increased at a rate of 15 °C min⁻¹ until it reached 250 °C and was maintained at this temperature for 3 min. The isotopic enrichment of each chemical was examined by EI-MS. The response factors for the isotopomers of these chemicals were within a small experimental error; thus, it was assumed that all the isotopomers would have identical response factors.

The attenuated total reflection Fourier transform infrared spectroscopy (ATR-FTIR) setup followed ref. [26]. The ATR-FTIR setup consisted of a Harrick Horizon multiple internal reflection accessory coupled to a 4 mL flow-through cell containing a ZnSe crystal on the bottom plate and a quartz window on the top plate. The 45° internal reflection element of 50 × 10 × 2 mm³ allowed approximately 11 infrared bounces. The Fourier transform infrared measurements were performed with a Nicolet 8700 FT-IR equipped with a DTGS detector.

Photocatalytic experiments for kinetic studies

The photocatalytic degradation reactions of the dicarboxylic acids for the kinetic studies were all performed in Pyrex vessels (50 mL) with a solution volume of 50 mL. The initial concentration for all the substrate dicarboxylic acids was 0.5 mM. P25 powder was added at 0.5 g L⁻¹. Irradiation was performed with a 100 W mercury lamp (Toshiba SHL-100UVQ-2), and the wavelength range was approximately 310 to 400 nm.

To reveal the redox nature of all the dicarboxylic acids used, we performed controlled experiments by using homogenous oxidation of persulfate (S₂O₈²⁻), during which UV irradiation was employed to homogeneously break the peroxide bonds and produce active SO₄^{•-} free radicals. This activation of S₂O₈²⁻ by UV irradiation could be compared with the TiO₂/UV photocatalysis in which the possible effects of direct photolysis by UV irradiation on the photocatalytic degradation of dicarboxylic acid might be offset. The kinetic studies concerning the photooxidation of dicarboxylic acids by persulfate ion (S₂O₈²⁻)^[22] were also all performed in Pyrex vessels (50 mL) with a solution volume of 50 mL. The initial concentration for all the substrate dicarboxylic acids was 0.5 mM, and the initial concentration of persulfate was 15 mM. The irradiation was also performed with a 100 W mercury lamp. The eluent was 15 mM KOH solution, the flow rate was 1.0 mL min⁻¹ in the IC analysis.

Photocatalytic tests for isotopic studies

All the isotope-labelling experiments, unless otherwise specified, were performed in Pyrex vessels (10 mL) with a solution volume of 8 mL. The initial concentration for all the substrate dicarboxylic acids was 5 mM, and 0.5 g L⁻¹ of P25 was added. Before use in the ¹⁸O₂ reaction, the solution in the vessel was placed under vacuum with a pump, purged with argon six times to remove air, and then was saturated with ¹⁸O₂. After the photocatalytic isotope-labelling reaction was stopped, the solution was extracted with ethyl ether three times. Then, the ethyl ether was silylated with silylating reagents (BSU and HMN). After centrifugation, the supernatant was removed and was analysed by GC-MS to give the oxygen isotopic profile in the target degraded products.

ATR-FTIR measurements

According to ref. [26], a layer of water was added dripwise onto the surface of the ZnSe crystal coated with a TiO₂ film, the crystal was scanned, and the background spectrum was obtained. Afterwards, the dicarboxylic acid solution was added dripwise onto the surface and the adsorption equilibrium with the TiO₂ film was attained (Figure 5).

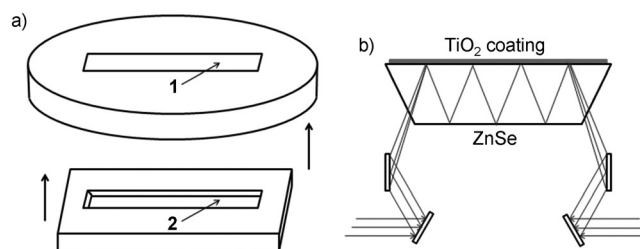


Figure 5. a) Schematic of the ATR-FTIR cell, including the quartz window on the top plate (1) and the internal reflection element on the bottom plate (2); b) Representation of the IR path and penetration into the TiO₂ coating. In practice, approximately 11 bounces were allowed by the crystal dimensions rather than the 4 bounces shown.

TiO₂ film preparation

P25 was suspended in distilled water at a concentration of 5 g L⁻¹. The suspension was treated for 1 h in a 40 kHz ultrasonic bath and then ground in an agate mortar for 30 min; 0.5 mL of this suspension was spread on the ZnSe crystal and was dried for 1 h at 100 °C. The conditions used formed uniform thick TiO₂ coatings that could be used in ATR-FTIR experiments.

Acknowledgements

We gratefully acknowledge the National Basic Research Program of China (973 program Nos. 2010CB933503, 2013CB632405), the National Science Foundation of China (Grant No. 21137004, 21077110, 21277147), and the Chinese Academy of Sciences for financial support.

Keywords: chelating coordination • decarboxylation • dicarboxylic acids • isotope labelling experiments • TiO₂-based photocatalysis

- [1] A. Fujishima, X. Zhang, D. A. Tryk, *Surf. Sci. Rep.* **2008**, *63*, 515–582.
- [2] R. Asahi, T. Morikawa, T. Ohwaki, K. Aoki, Y. Taga, *Science* **2001**, *293*, 269–271.
- [3] a) P. Pichat, *Photocatalysis and water purification*, Wiley-VCH, Weinheim, **2013**; b) M. R. Hoffmann, S. T. Martin, W. Y. Choi, D. W. Bahnemann, *Chem. Rev.* **1995**, *95*, 69–96.
- [4] a) M. A. Henderson, *Surf. Sci. Rep.* **2011**, *66*, 185–297; b) A. L. Linsebigler, G. Lu, J. T. Yates, *Chem. Rev.* **1995**, *95*, 735–758.
- [5] S. H. Szczepankiewicz, A. J. Colussi, M. R. Hoffmann, *J. Phys. Chem. B* **2000**, *104*, 9842–9850.
- [6] R. B. Draper, M. A. Fox, *Langmuir* **1990**, *6*, 1396–1402.
- [7] T. Sumita, T. Yamaki, S. Yamamoto, A. Miyashita, *Appl. Surf. Sci.* **2002**, *200*, 21–26.
- [8] P. Fernández-Ibáñez, J. Blanco, S. Malato, F. J. de Las Nieves, *Water Res.* **2003**, *37*, 3180–3188.
- [9] a) B. Wen, Y. Li, C. Chen, W. Ma, J. Zhao, *Chem. Eur. J.* **2010**, *16*, 11859–11866; b) Y. Li, B. Wen, C. Yu, C. Chen, H. Ji, W. Ma, J. Zhao, *Chem. Eur. J.* **2012**, *18*, 2030–2039.
- [10] D. F. Ollis, E. Pelizzetti, N. Serpone, *Environ. Sci. Technol.* **1991**, *25*, 1522–1529.
- [11] G. A. Russell, *J. Am. Chem. Soc.* **1957**, *79*, 3871–3877.
- [12] a) S. Yurdakal, G. Palmisano, V. Loddo, V. Augugliaro, L. Palmisano, *J. Am. Chem. Soc.* **2008**, *130*, 1568–1569; b) M. Zhang, C. Chen, W. Ma, J. Zhao, *Angew. Chem.* **2008**, *120*, 9876–9879; *Angew. Chem. Int. Ed.* **2008**, *47*, 9730–9733; c) A. M. Khenkin, R. Neumann, *J. Am. Chem. Soc.* **2008**, *130*, 14474–14476; d) M. Zhang, Q. Wang, C. Chen, L. Zang, W. Ma, J. Zhao, *Angew. Chem.* **2009**, *121*, 6197–6200; *Angew. Chem. Int. Ed.* **2009**, *48*, 6081–6084.
- [13] T. Ohno, S. Izumi, K. Fujihara, Y. Masaki, M. Matsumura, *J. Phys. Chem. B* **2000**, *104*, 6801–6803.
- [14] N. Serpone, J. Martin, S. Horikoshi, H. Hidaka, *J. Photochem. Photobiol. A* **2005**, *169*, 235–251.
- [15] a) B. Kraeutler, A. J. Bard, *J. Am. Chem. Soc.* **1978**, *100*, 5985–5992; b) M. A. Fox, M. T. Dulay, *Chem. Rev.* **1993**, *93*, 341–357.
- [16] J. Schwitzgebel, J. G. Ekerdt, H. Gerischer, A. Heller, *J. Phys. Chem.* **1995**, *99*, 5633–5638.
- [17] T. D. Bui, A. Kimura, S. Ikeda, M. Matsumura, *J. Am. Chem. Soc.* **2010**, *132*, 8453–8458.
- [18] R. R. Sever, T. W. Root, *J. Phys. Chem. B* **2003**, *107*, 10521–10530.
- [19] a) I. Dolamic, T. Bürgi, *J. Phys. Chem. B* **2006**, *110*, 14898–14904; b) R. Enriquez, A. G. Agrios, P. Pichat, *Catal. Today* **2007**, *120*, 196–202.
- [20] a) I. Dolamic, T. Bürgi, *J. Catal.* **2007**, *248*, 268–276; b) W. Irawaty, D. Friedmann, J. Scott, P. Pichat, R. Amal, *Catal. Today* **2011**, *178*, 51–57; c) Q. Chen, J. M. Song, F. Pan, F. L. Xia, J. Y. Yuan, *Environ. Technol.* **2009**, *30*, 1103–1109.
- [21] The degradation of oxalic acid was seemingly an exception. We believe that the singular degradation of oxalic acid partly originated from direct UV-light photolysis because of the typical instability of oxalic acid and that this photolysis may conceal a slower photocatalytic rate than that of propanedioic acid (Figure 1a). Thus, we conducted control experiments for direct photocatalysis, and indeed found that oxalic acid partly degraded under the UV-light irradiation used. After correlation with the control value, the genuine photocatalytic degradation rate of oxalic acid was not faster than that of propanedioic acid. For CO₂ formation, the mineralisation rate of oxalic acid was not correlated with the control mineralisation experiment.
- [22] B. B. Wang, M. H. Cao, Z. J. Tan, L. L. Wang, S. H. Yuan, J. Chen, *J. Hazard. Mater.* **2010**, *181*, 187–192.
- [23] J. Yang, C. Chen, H. Ji, W. Ma, J. Zhao, *J. Phys. Chem. B* **2005**, *109*, 21900–21907.
- [24] S. Kang, B. Xing, *Langmuir* **2007**, *23*, 7024–7031.
- [25] N. J. Nicholas, G. V. Franks, W. A. Ducker, *Langmuir* **2012**, *28*, 7189–7196.
- [26] A. R. Almeida, J. A. Moulijn, *J. Phys. Chem. C* **2008**, *112*, 1552–1561.
- [27] H. Gerischer, A. Heller, *J. Phys. Chem.* **1991**, *95*, 5261–5267.
- [28] X. Li, J. W. Cubbage, T. A. Tetzlaff, W. S. Jenks, *J. Org. Chem.* **1999**, *64*, 8509–8524.
- [29] L. F. Liao, C.-F. Lien, D.-L. Shieh, M.-T. Chen, J.-L. Lin, *J. Phys. Chem. B* **2002**, *106*, 11240–11245.
- [30] R. A. Marcus, *J. Chem. Phys.* **1956**, *24*, 966; R. A. Marcus, *Annu. Rev. Phys. Chem.* **1964**, *15*, 155.
- [31] a) C. Xu, W. Yang, Q. Guo, D. Dai, M. Chen, X. Yang, *J. Am. Chem. Soc.* **2013**, *135*, 10206–10209; b) M. Shen, D. P. Acharya, Z. Dohnálek, M. A. Henderson, *J. Phys. Chem. C* **2012**, *116*, 25465–25469.

Received: August 16, 2013

Published online on January 8, 2014